

The effect of transducer directivity on time reversal focusing

Brian E. Anderson, Miles Clemens, and Matthew L. Willardson

Citation: *The Journal of the Acoustical Society of America* **142**, EL95 (2017); doi: 10.1121/1.4994688

View online: <http://dx.doi.org/10.1121/1.4994688>

View Table of Contents: <http://asa.scitation.org/toc/jas/142/1>

Published by the *Acoustical Society of America*

The effect of transducer directivity on time reversal focusing

Brian E. Anderson,^{a)} Miles Clemens, and Matthew L. Willardson
Acoustics Research Group, Department of Physics and Astronomy, Brigham Young University, Provo, Utah 84602, USA
bea@byu.edu, theexperiment113@gmail.com, mwillardson@verizon.net

Abstract: This letter explores the effect of the directivity of a source on time reversal acoustic focusing of energy. A single loudspeaker produces an airborne focus of sound in a reverberation chamber and in a classroom. Individual foci are created at microphone positions that surround the loudspeaker. The primary axis of the loudspeaker is then rotated and experiments are repeated to average out the room response. Focal amplitude, temporal quality of the foci, and spatial focusing quality are compared to determine the optimal angle to aim a directional source axis relative to the desired focal position.

© 2017 Acoustical Society of America

[DHC]

Date Received: May 19, 2017 **Date Accepted:** July 6, 2017

1. Introduction

Time reversal (TR) is a signal processing technique that can be used to focus sound to a location in space for source reconstruction, communication, and intentional sound focusing.^{1,2} TR is a two-step process consisting of a forward step in which an impulse response is determined between two locations, and a backward step where the impulse response is reversed in time and broadcast from one location, which results in a spatial focus of energy at the other location. Several sources may be used, each with a unique impulse response, to form a so called time reversal mirror (TRM).³ The first known use of TR technology was for underwater communications between two vessels (at the time it was called a matched signal technique).^{4,5} This early experiment utilized what has been termed reciprocal time reversal (RTR),² where a signal is broadcast from location A, a recording of the signal is made at location B, this recording is then flipped in time, sent electronically to location A, subsequently broadcast from location A, and a TR focus is then created at location B. Subsequently, researchers have named the technique time reversal acoustics and have recently applied it to underwater communications,^{6,7} medical applications,^{8,9} nondestructive evaluation,¹⁰⁻¹³ and infrasound.¹⁴

TR focusing is typically done with impulsive signals, though focusing of continuous wave signals has been demonstrated.¹⁵ The focusing provided by TR results from the constructive interference of emissions from some combination of real sources and virtual sources. The real sources are the number of TRM elements and the virtual sources are the result of appropriately timed scattering, whose timing is encoded in the reversed impulse response(s). This TR focus is localized in space and provides a reconstruction of the original signal that was broadcast in the forward step. The forward step to obtain impulse response(s) may be obtained experimentally or numerically, and the backward propagation may also be done experimentally or numerically depending on the application.

The purpose of this paper is to determine how a directional source axis should be aimed with respect to a desired focal location in a TR experiment, assuming that location is generally known. Experiments are conducted in a reverberation chamber and a medium-sized classroom, along with some benchmark experiments conducted in an anechoic chamber. A single loudspeaker is used with RTR to create foci individually at various target focal locations (target microphones) that are at varying angles with respect to the loudspeaker's axis. In the reverberation chamber, seemingly paradoxically, the maximal focusing amplitude is generated when the loudspeaker is facing away from the target microphone, whereas the focal amplitude in the classroom is fairly independent of the loudspeaker's axis with respect to the target microphone. Temporal and spatial quality of the TR focusing is maximal with the loudspeaker facing the target microphone.

^{a)} Author to whom correspondence should be addressed.

2. Experiment setup

Two rooms were selected for the TR experiments that have very different reverberation times, but with similar room volumes. In the process described below, 64 impulse responses were obtained, from which the average reverberation time could be determined. Reverse Schroeder integration¹⁶ (*RSI*) is performed on each impulse response and the decay rate is extracted from the *RSI* between the -5 to -35 dB down points (down from the initial peak in the *RSI*) on the curve as specified by room acoustics standards.¹⁶ The *RT60* value is then twice the time it took to decay the 30 dB between the -5 and -35 dB points. The first room is a reverberation chamber measuring $4.96\text{ m} \times 5.89\text{ m} \times 6.98\text{ m}$ with a volume of 204 m^3 . The average *RT60* for the reverberation chamber is 6.89 s, resulting in a Schroeder frequency¹⁷ of 385 Hz. The second room is a standard classroom measuring $6.30\text{ m} \times 10.41\text{ m} \times 3.27\text{ m}$ with a volume of 214 m^3 . The average *RT60* for the classroom is 0.65 s, resulting in a Schroeder frequency of 115 Hz. Finally an anechoic chamber with working dimensions $8.71\text{ m} \times 5.66\text{ m} \times 5.74\text{ m}$ is also used. Figures 1(a) and 1(b) contain photographs of the reverberation chamber and classroom with the equipment setup in them.

For a given room under test, a Mackie HR824mk1 (Woodinville, WA) loudspeaker is placed on a stand such that the center of the loudspeaker is at a height of 1.63 m above the floor. The measured directivity (logarithmically averaged over frequency between 800 Hz and 10 kHz) for this loudspeaker, as measured in the horizontal plane in an anechoic chamber, is shown in Fig. 3(a). The directivity factor¹⁸ along the loudspeaker axis is 3.71. Eight PCB 377B02 (Depew, NY) microphones with Larson Davis PRM426 (Provo, UT) preamplifiers are placed 1.5 m away from the loudspeaker at 45° angles with respect to one another on microphone stands at a height of 1.63 m. All microphones are at least 1 m from any wall. Random incidence caps were fitted onto these normally free-field microphones since we expect the sound focusing to come in from all directions. The microphones were placed with a slight ($\sim 5^\circ$) rotation relative to the room walls, meaning that no axis connecting two microphones and the loudspeaker is perpendicular to the room walls. Figures 1(c) and 1(d) display drawings of the cross sections of the reverberation chamber and the classroom with the loudspeaker and microphone positions denoted. The loudspeaker is placed on an Outline ET250-3D (Farmingdale, NY) turntable with the initial $\phi = 0^\circ$ axis of the loudspeaker denoted by the red colored arrows in Figs. 1(c) and 1(d). $\theta = 0^\circ$ is the

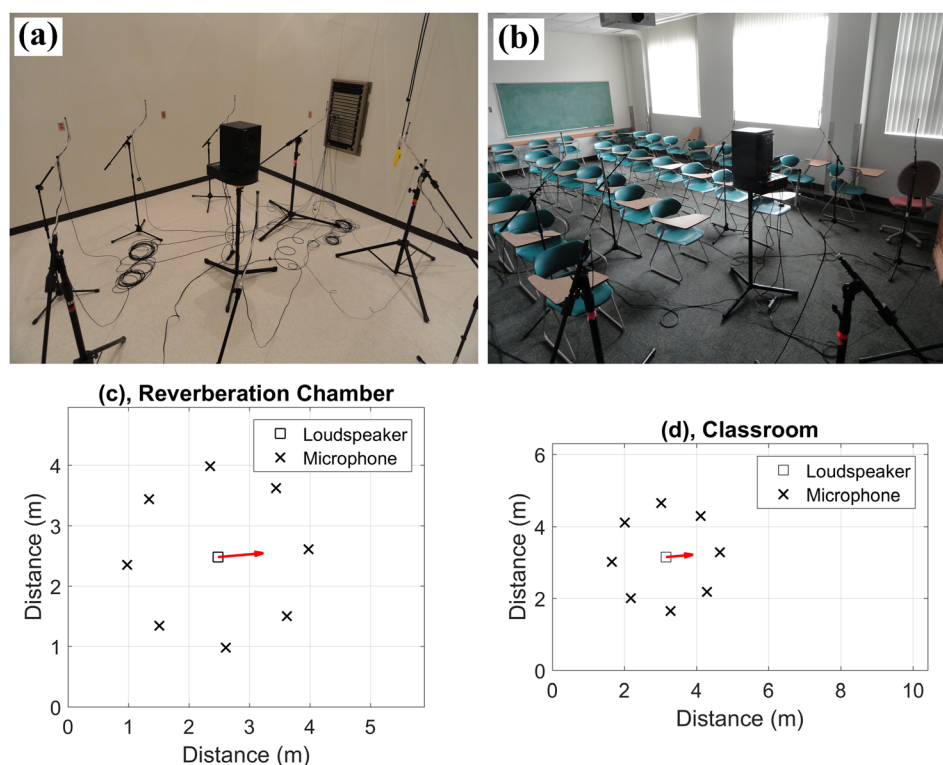


Fig. 1. (Color online) Information about the experiments conducted in this paper. (a) and (b) Photographs of the setups in the reverberation chamber and medium-sized classroom, respectively. (c) and (d) Drawings of the setups in the reverberation chamber and classroom in plane view, respectively. The loudspeaker's axis is denoted by the arrow.

angle of the loudspeaker axis, which will be rotated in the experiments. Thus 0° for θ is not always the same as 0° for ϕ . The axis of rotation is clockwise as pictured. θ_0 is used to denote the angle of the target microphone with respect to the current loudspeaker axis angle and is the main angle used in the results in Fig. 3, while the seven angles, $\theta_1, \theta_2, \theta_3, \dots, \theta_7$, are the away microphone locations.

To understand how well time reversal is able to focus sound energy to locations in the room at different angles with respect to the primary axis of the loudspeaker, eight separate time reversal experiments are conducted with the loudspeaker's primary axis held fixed pointing at one of the microphones. The full-time reversal experiment with forward and backward steps is conducted to focus sound at each of the eight microphones, while recording at the other seven away microphones for each of the eight experiments. This set of experiments allows quantification of the effect of the directional nature of a single loudspeaker on time reversal focusing in a room. In an attempt to remove any directional effects that the room has on these experiments, the loudspeaker is then rotated 45° and the full set of experiments described previously in this paragraph is again conducted. This set of experiments are then conducted with a loudspeaker rotation of 90° and so on for each of the eight independent 45° angle axes of rotation. In each of these sets of experiments, the coordinate system of the microphones (θ_0 and $\theta_1, \theta_2, \theta_3, \dots, \theta_7$) is also rotated, such that in total there are eight individual time reversal experiments with the loudspeaker's primary axis (redefined as $\theta = 0^\circ$) facing a target microphone directly in front of it ($\theta_0 = 0^\circ$). Similarly, there are a total of eight individual time reversal experiments with the loudspeaker's primary axis facing in the opposite direction as the target microphone ($\theta_0 = 180^\circ$) and for every other 45° angle. In total, $8 \times 8 = 64$ focal signals are recorded at target microphones and $7 \times 8 \times 8 = 448$ signals are recorded at away microphones. This set of measurements is done for both the reverberation chamber and for the classroom.

During the forward step of the time reversal process, a burst chirp signal, $s(t)$, spanning 800–10 000 Hz is broadcast from the loudspeaker and recorded by the selected target microphone, $r(t)$. A National Instruments PXI-1042Q (Austin, TX) chassis with a PXI-4462 digitizer card (24 bit resolution) and a sampling frequency of 44.1 kHz is used. The output signals are sent through the headphone jack of a PC computer to the self-amplified loudspeaker. An internally developed program (using LabVIEW from National Instruments) was used to control the experiments. A cross correlation of $s(t)$ and $r(t)$ results in a signal that may be used in place of a direct measurement of the impulse response, $ir(t)$, between the loudspeaker and the target microphone at θ_0 . The cross correlation operation yields an amplitude scaled version of the band-limited impulse response when $s(t)$ has a flat frequency response. During the backward step of the time reversal process, the impulse response is then reversed in time [see Fig. 2(a) for an example signal], $ir(-t)$, normalized to the maximum input allowed for the amplifier, amplified, and is then broadcast from the loudspeaker and recorded by all eight microphones, producing a focus signal, $f_{\theta_0}(t)$, at the target microphone [see Fig. 2(b) for an example signal], and unfocused signals, $a_{\theta_1, \dots, \theta_7}(t)$, at the other seven “away” microphones [see Fig. 2(b) for an example signal].

The example signals displayed in Figs. 2(a) and 2(b) are representative of those obtained when the loudspeaker's primary axis is pointing at the target microphone in the reverberation chamber ($\theta_0 = 0^\circ$). If the target microphone is instead selected as the microphone $\theta_0 = 180^\circ$ relative to the loudspeaker's primary axis, then one obtains Figs. 2(c) and 2(d) for the reversed impulse response and signals during focusing, respectively. Note that the peak pressure is 2.8 times higher when the loudspeaker is facing away from the target microphone than when it is facing the target microphone. However, the peak pressure for the away microphones shown is 2.9 times (8.9 dB) higher when the loudspeaker is facing away from the target microphone than when the loudspeaker is facing towards the target microphone. Thus, in the cases shown, while the focal amplitude increases when the loudspeaker is facing away from the target, the amplitude elsewhere in the room also increases by a similar amount. Looking at the signals sent to the loudspeaker in each of these two cases, depicted in Figs. 2(a) and 2(c), one can see that the signal in Fig. 2(c) contains more amplitude over time than the signal in Fig. 2(a) (recall that these signals are normalized with respect to their peaks). The large spike in Fig. 2(a) is from the direct arrival, which dominates the impulse response and correspondingly arrives at the target microphone with a large amplitude. In the case of Fig. 2(d), the loudspeaker is facing away from the target microphone so the direct signal is weaker due to the differences in the directivity of the amplitude projected from the front of the loudspeaker versus the rear of the loudspeaker. These types of observations will be explored further in this paper.

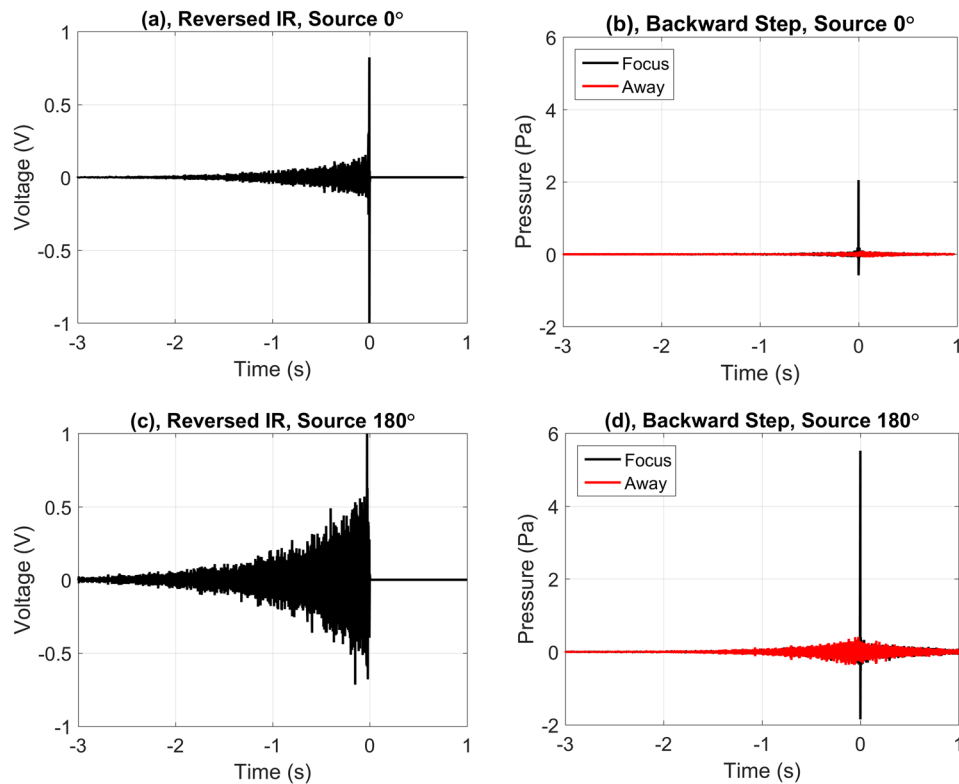


Fig. 2. (Color online) Examples of time reversal focusing signals in the reverberation chamber. (a) and (c) display the reversed impulse responses when the loudspeaker's axis is pointed at 0° and at 180° , respectively. (b) and (d) display the focal signals and sample away signals when the loudspeaker's axis is pointed at 0° and at 180° , respectively.

In order to quantify the focusing performance of the time reversal process, several metrics are computed. The first is the squared peak focal amplitude at the target microphone, averaged across the rotation of the loudspeaker axis (angular average denoted by $\langle \cdot \rangle_\phi$) to obtain a value at each of the eight θ_0 values ($\theta_0 = -180^\circ, -135^\circ, -90^\circ, -45^\circ, 0^\circ, 45^\circ, 90^\circ, 135^\circ, 180^\circ$)

$$p_{P,F}^2(\theta_0) = \langle \max\{f_{\theta_0,\phi}^2(n)\} \rangle_\phi, \quad (1)$$

where n is the sample number and is used in place of continuous time for a recorded signal. The second metric is the temporal quality of the TR focal signal,¹⁹ $f_{\theta_0,\phi}(n)$, at the target microphone, again averaged across the rotation angle ϕ of the loudspeaker axis,

$$\xi_T(\theta_0) = \frac{p_{P,F}^2(\theta_0)}{\left\langle \frac{T}{N} \sum_{n=1}^N f_{\theta_0,\phi}^2(n) \right\rangle_\phi}, \quad (2)$$

where N is the number of time samples in $f_{\theta_0,\phi}(n)$ and T is the length of $f_{\theta_0,\phi}(n)$ in time. The third metric is the peak amplitude among all of the other seven away microphones at angles $\theta_1, \theta_2, \dots, \theta_7$, with the away signals denoted by $a_{\theta_i,\phi}(n)$, which is also averaged over ϕ ,

$$p_{P,A}^2(\theta_0) = \left\langle \max \begin{bmatrix} \max\{a_{\theta_1,\phi}^2(n)\} \\ \dots \\ \max\{a_{\theta_7,\phi}^2(n)\} \end{bmatrix} \right\rangle_\phi, \quad (3)$$

where the inner maximum function, $\max\{\cdot\}$, is a maximum over time and the outer maximum function, $\max[\cdot]$, is a maximum over away microphone signal maxima. To determine the quality of the time reversal focusing as a function of space, we can compare the peak focal amplitudes at the target microphone to the average peak amplitudes recorded at away microphones

$$Q_P(\theta_0) = 10 \log_{10} \frac{p_{P,F}^2(\theta_0)}{p_{P,A}^2(\theta_0)}. \quad (4)$$

This last metric illustrates how significant the focal peak is compared to the pressure amplitudes at other locations in the room, proving a measure of the focusing of the sound as a function of space.

As mentioned previously the directivity of the loudspeaker is measured in the anechoic chamber. A single TR experiment is conducted with the loudspeaker's axis facing a target microphone to extract a direct sound amplitude. TR at target locations other than at 0° are simulated using the directivity and assuming no reflections from the room.

3. Results and discussion

Figure 3(a) displays the average focal amplitude $20 \log_{10}[p_{P,F}^2(\theta_0)]$ at each target microphone position θ_0 . Note that the reverberation chamber consistently yields the highest $p_{P,F}^2(\theta_0)$, at any target microphone, of any of the three rooms due to the strength of the virtual sources (low absorption coefficients on the walls, floor, and ceiling). The classroom yields higher $p_{P,F}^2(\theta_0)$, at any target microphone, than the anechoic chamber since the anechoic chamber only utilizes the direct sound (no contribution from virtual sources). Interestingly, the $p_{P,F}^2(\theta_0)$ is largest for the reverberation chamber at $\theta_0 = 180^\circ$ and the lowest $p_{P,F}^2(\theta_0)$ at $\theta_0 = 0^\circ$ (9.8 dB lower than at $\theta_0 = 180^\circ$). The classroom yields much more consistent $p_{P,F}^2(\theta_0)$ irrespective of θ_0 , with only 2.4 dB variation, but at $\theta_0 = 180^\circ$, the $p_{P,F}^2(\theta_0)$ is largest. Since the anechoic chamber can only utilize the direct sound, $p_{P,F}^2(\theta_0)$ is simply the directivity of the loudspeaker at a 1.5 m distance from the source. At $\theta_0 = 0^\circ$ the virtual sources in the reverberation chamber contribute 14.3 dB gain to $p_{P,F}^2(\theta_0)$, whereas the virtual sources in the classroom contribute 4.3 dB gain to $p_{P,F}^2(\theta_0)$. At $\theta_0 = 180^\circ$ the virtual sources in the reverberation chamber contribute 39.7 dB gain to $p_{P,F}^2(\theta_0)$, whereas the virtual sources in the classroom contribute 20.6 dB gain to $p_{P,F}^2(\theta_0)$. Finally the reverberation chamber provides a 10 dB gain in $p_{P,F}^2(\theta_0)$ relative to the classroom at $\theta_0 = 180^\circ$ and a 19.1 dB gain in $p_{P,F}^2(\theta_0)$ at $\theta_0 = 0^\circ$. Thus in reverberant environments, pointing the loudspeaker away from the focal location yields the highest amplitude, in contrast to the gain provided by the loudspeaker's directivity.

Figure 3(b) displays the square root of the temporal quality, $\sqrt{\xi_T(\theta_0)}$, as a function of θ_0 . The square root helps identify the average linear factor by which the focal amplitude is larger than the average signal magnitude. In both the reverberation chamber and the classroom, the $\sqrt{\xi_T(\theta_0)}$ peaks at $\theta_0 = 0^\circ$ and is minimal at

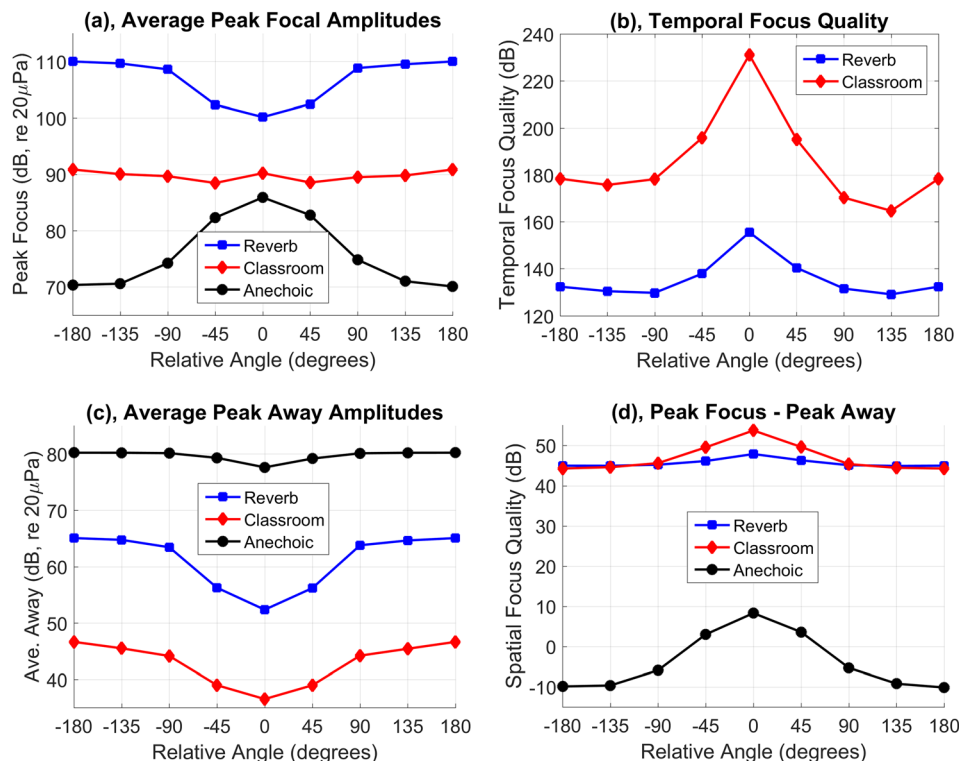


Fig. 3. (Color online) Metrics used to quantify the effects of the angle of the loudspeaker's axis relative to the focal location (the x axis in each of the plots). A brief description of each plot is given in its title.

$\theta_0 = \pm 135^\circ$. The reverberation chamber has a 23% higher $\sqrt{\xi_T(\theta_0)}$ at $\theta_0 = 0^\circ$ versus at $\theta_0 = 180^\circ$ while the classroom yields a 15% higher $\sqrt{\xi_T(\theta_0)}$ at $\theta_0 = 0^\circ$ versus at $\theta_0 = 180^\circ$. Thus the $\sqrt{\xi_T(\theta_0)}$ is highest when the loudspeaker is pointed at the focal location. Data from the anechoic chamber is not included here since $\sqrt{\xi_T(\theta_0)}$ would be very high, owing to the sole presence of the direct sound.

Figure 3(c) displays the average away amplitude $20 \log_{10}[p_{P,A}^2(\theta_0)]$. The $p_{P,A}^2(\theta_0)$ is highest at $\theta_0 = 180^\circ$ and is lowest at $\theta_0 = 0^\circ$. For the reverberation chamber the difference between the $p_{P,A}^2(\theta_0)$ at $\theta_0 = 180^\circ$ compared to the $p_{P,A}^2(\theta_0)$ at $\theta_0 = 0^\circ$ is 12.7 dB. For the classroom, this difference is 10.1 dB. Finally, for the anechoic chamber, this difference is 2.6 dB. Thus while the $p_{P,F}^2(\theta_0)$ is highest at $\theta_0 = 180^\circ$, the $p_{P,A}^2(\theta_0)$ is also highest at that angle.

Figure 3(d) displays the difference between $p_{P,F}^2(\theta_0)$ and $p_{P,A}^2(\theta_0)$ in the form of the spatial quality metric, $Q_P(\theta_0)$. The reverberation chamber yields a 2.9 dB gain in $Q_P(\theta_0)$ at $\theta_0 = 0^\circ$ relative to $\theta_0 = 180^\circ$. The classroom yields a 9.5 dB gain in $Q_P(\theta_0)$ for the same angles. Interestingly, at $\theta_0 = 180^\circ$ the $Q_P(\theta_0)$ is only different by a factor of 0.7 dB when comparing the reverberation chamber and the classroom, whereas it is different by a factor of 5.9 dB at $\theta_0 = 0^\circ$. In the anechoic chamber, where TR with a single source does not make sense, the $Q_P(\theta_0)$ is positive valued when the target is in the forward $> \pm 45^\circ$.

During the backward step of the TR process, if a directional loudspeaker is pointed away from the target focusing location (i.e., the target microphone) the direct sound arrival at the target microphone is reduced because the loudspeaker's primary axis of radiation is pointing away from the target microphone. The strongest radiation from the loudspeaker then must reflect off of a wall, or scatterer, before it arrives at the target microphone, undergoing geometric spreading and losing some energy through its interaction with the wall. Often the reversed impulse response is normalized prior to broadcast in the backward step to maximize the output of the amplifier. The amplitude of the reflected sound in the impulse response relative to the direct sound is the key. In contrast, when the loudspeaker is pointed towards the target microphone, the direct sound dominates the impulse response and therefore dominates the normalized, reversed impulse response. When the room wall's absorption coefficient is higher, such as in the classroom, the reflected sound (from images sources) does not contribute to as large of a focal amplitude as it does for the reverberation chamber.

4. Conclusions

The transducer directivity of a source can greatly impact focal amplitude of time reversal (TR) focusing and the temporal and spatial quality of that focusing. Larger focal amplitude can be obtained by pointing a directional source axis away from the intended target focal location. However, the focal signal at the target location can be made more impulsive in nature (higher temporal focal quality) if the source axis is pointed towards the target location. Additionally, the ability of TR to focus more amplitude to the target location instead of other locations (spatial focusing quality) is also enhanced by pointing the source axis towards the target location. Thus, a tradeoff exists between overall focal amplitude being achieved when the source axis is pointing away from the target location while the spatial and temporal quality of the focusing is optimal when the source axis is pointing towards the target location. These findings have implications for TR applications in which the target location is either known or some knowledge exists about the direction of the target location relative to each source used.

Acknowledgments

We gratefully acknowledge internal support from College of Physical and Mathematical Sciences and the Department of Physics and Astronomy at Brigham Young University.

References and links

- ¹M. Fink, "Time reversed acoustics," *Phys. Today* **50**(3), 34–40 (1997).
- ²B. E. Anderson, M. Griffa, C. Larmat, T. J. Ulrich, and P. A. Johnson, "Time reversal," *Acoust. Today* **4**(1), 5–16 (2008).
- ³M. Fink, D. Cassereau, A. Derode, C. Prada, P. Roux, and M. Tanter, "Time-reversed acoustics," *Rep. Prog. Phys.* **63**(12), 1933–1995 (2000).
- ⁴A. Parvulescu and C. Clay, "Reproducibility of signal transmission in the ocean," *Radio Electron. Eng.* **29**, 223–228 (1965).
- ⁵C. S. Clay and B. E. Anderson, "Matched signals: The beginnings of time reversal," *Proc. Mtgs. Acoust.* **12**, 055001 (2011).

- ⁶S. M. Jesus, S. I. Siddiqui, and A. Silva, "Path specific Doppler compensation in time-reversal communications," *J. Acoust. Soc. Am.* **137**(4), EL300–EL306 (2015).
- ⁷H. C. Song and W. S. Hodgkiss, "Self-synchronization and spatial diversity of passive time reversal communication (L)," *J. Acoust. Soc. Am.* **137**(5), 2974–2977 (2015).
- ⁸M. Fink, "Time-reversal acoustics in biomedical engineering," *Ann. Rev. Biomed. Eng.* **5**(1), 465–497 (2003).
- ⁹S. Dos Santos and Z. Prevorovsky, "Imaging of human tooth using ultrasound based chirp-coded nonlinear time reversal acoustics," *Ultrason.* **51**(6), 667–674 (2011).
- ¹⁰C. Prada, E. Kerbrat, D. Cassereau, and M. Fink, "Time reversal techniques in ultrasonic nondestructive testing of scattering media," *Inv. Problems* **18**(6), 1761–1773 (2002).
- ¹¹B. E. Anderson, M. Griffa, T. J. Ulrich, P.-Y. Le Bas, R. A. Guyer, and P. A. Johnson, "Crack localization and characterization in solid media using time reversal techniques," in *44th US Rock Mechanics Symposium and 5th U.S.-Canada Rock Mechanics Symposium*, Salt Lake City, UT (June 2010).
- ¹²E. L. Villaverde, S. Robert, and C. Prada, "Ultrasonic imaging of defects in coarse-grained steels with the decomposition of the time reversal operator," *J. Acoust. Soc. Am.* **140**(1), 541–550 (2016).
- ¹³B. E. Anderson, L. Pieczonka, M. C. Remillieux, T. J. Ulrich, and P.-Y. Le Bas, "Stress corrosion crack depth investigation using the time reversed elastic nonlinearity diagnostic," *J. Acoust. Soc. Am.* **141**(1), EL76–EL81 (2017).
- ¹⁴J. B. Lonzaga, "Time reversal for localization of sources of infrasound signals in a windy stratified atmosphere," *J. Acoust. Soc. Am.* **139**(6), 3053–3062 (2016).
- ¹⁵B. E. Anderson, R. A. Guyer, T. J. Ulrich, and P. A. Johnson, "Time reversal of continuous-wave, steady-state signals in elastic media," *Appl. Phys. Lett.* **94**(11), 111908 (2009).
- ¹⁶ISO 3382:1997(E), *Acoustics-Measurement of the Reverberation Time of Rooms with Reference to other Acoustical Parameters* (International Organization for Standardization, Geneva, Switzerland, 1997).
- ¹⁷M. R. Schroeder and K. H. Kuttruff, "On frequency response curves in rooms. Comparison of experimental, theoretical, and Monte Carlo results for the average frequency spacing between maxima," *J. Acoust. Soc. Am.* **34**(1), 76–80 (1962).
- ¹⁸L. L. Beranek, *Acoustics* (Acoustical Society of America, New York, 1993), pp. 163–164.
- ¹⁹C. Heaton, B. E. Anderson, and S. Young, "Time reversal focusing of elastic waves in plates for an educational demonstration," *J. Acoust. Soc. Am.* **141**(2), 1084–1092 (2017).